Turkish Journal of Engineering
https://dergipark.org.tr/en/pub/tuje
e-ISSN 2587-1366

Determination of optimum design parameters of glow plug and experimental verification

Muciz Özcan [*1], **Muhammed Fahri Ünlerşen** [1], **Mehmet Şen** [2]

[1]*Necmettin Erbakan University, Department of Electric and Electronics, Türkiye*
[2]*Social Sciences University of Ankara, Distance Education Application and Research Center, Türkiye*

Keywords
Glow plug
Mutually inductance
Resistive element
Thermal imaging

Research Article
DOI: 10.31127/tuje.1062681

Received: 25.01.2022
Accepted: 10.03.2022
Published: 26.04.2022

Abstract

In Diesel Engines, the heat energy obtained from the glow plug increases the engine's ability to start up in cold climatic conditions and significantly reduces emissions of harmful gases leaving the exhaust. In cold climatic conditions, before the start off of diesel vehicles it is necessary to wait for about 10 s the cylinder block heating. This period negatively affects driving comfort. In this study, the mathematical results of the processes to optimize the time required for the glow plug to reach the required temperature have been experimentally proven. A test apparatus was developed to confirm experimentally the theoretical results. Thanks to these improvements concerning the manufacture of the glow plug, the time period to reach 850 ° C has been reduced by approximately 5 s. The proposed design is in accordance with the glow plug present in the market. Currently the whole glow plug must be changed at the end of lifetime, with our improvement only the inner tube resistance can be easily changed involving a cost reduction by about 60%.

1. Introduction

Diesel engines are becoming increasingly widespread in transportation and freight transport due to their high efficiency and development torque [1-3]. They have an internal combustion ignition system where fuel is sprayed on compressed air heated at approximately 700 °C - 900 °C inside the cylinder. In cold climate countries among the numerous problems that can affect the operation of diesel vehicles, one of the most important is the start off. Especially in the winter months, the cold engine block prevents the first run. In fact, the external low temperature affects the temperature of the cylinder block, which must be preheated to trig the fuel ignition [4-5]. The unburned mixture with a high fuel mixture ratio is release to atmosphere by the exhaust. Gas released to the atmosphere causes the release of toxic greenhouse gases to the environment [6-10]. At this moment, the burning event does not take place properly causing engine knockings [11]. In order avoid the mechanical abrasions between the motor and the transmission components and also to improve the driving comfort, diesel vehicles use a Glow Plug (GP).

Before the diesel engine start off, the heating element within the GP must be activated during about 10 to 20 s depending on the volume of combustion chambers. At the end of this time, the tip surface of the GP reaches a temperature between about 800 to 1000 °C allowing a comfortable engine start [12]. By using the GP, the smoke released from the engine during the start off is reduced from about 49 % to 60% [13-14]. Since the GP transforms the electrical energy of the battery to a thermal energy, prolonging the preheating temperature is shortening the lifetime of the car battery.

The diesel engine consists on at least four-cylinder blocks which contains a separate GP. Each of them must have the same properties to allow approximately the same ignition conditions for insuring the driving comfort. If not mechanical snags and exhaust gas emissions can be occurred.

In this study, GP used in diesel cars using 12 V supply voltage was targeted and product improvement studies that can be done in GP manufacturing.

* **Corresponding Author**

*(mozcan@erbakan.edu.tr) ORCID ID 0000-0001-5277-6650
(mfunlersen@erbakan.edu.tr) ORCID ID 0000-0001-7850-6712
(mehmet.sen@asbu.edu.tr) ORCID ID 0000-0001-7609-2210

Cite this article

Özcan, M., Ünlerşen, M. F., & Şen, M. (2023). Determination of optimum design parameters of glow plug and experimental verification. Turkish Journal of Engineering, 7(2), 125-133

2. Technical Background of GP

The GP contains four main elements; Glowing Tube (GT), Electrical Insulator (between heating resistance and GT), Insulator Ring (between connection terminal and body) and Heating Element (HE). The former consists of Heating Resistor (HR) and a Regulating Resistor (RR). These parts are shown in Fig. 1.

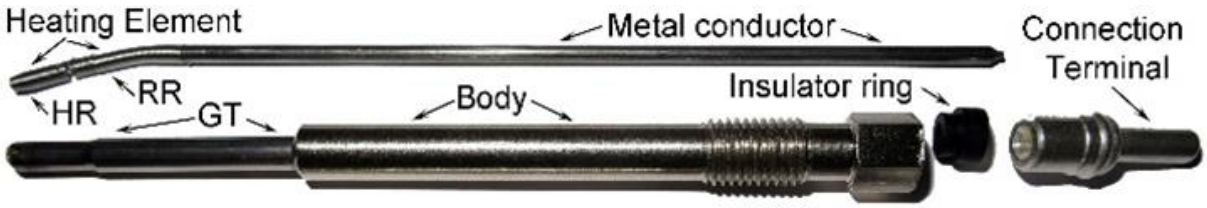

Figure 1. The basic parts of the GP and the assembly sequence

2.1. Selection of GT Material

The most important task of GT is to transfer the heat coming from the HR into the engine block with the lowest energy loss. This is the most important feature expected from GT in GPs. During the engine working, the GT must be resisted to high the internal temperature (1500-2000°C) and without being corroded.

In order to switch on and to enable the working of the HE (positive), the GP is connected the chassis (negative). For this reason, the protective sheath must be an electrically conductive material. A hollow rod tube made of Inconel ASTM / UNS 310 / 310S stainless steel material was selected as material meeting the requirements specified in this study. Physical properties of 310S Stainless Steel are in Table 1 [15]. If the protective sheath is an insulating material (e.g., ceramics), it must be removed from the protective jacket and must be connected at both ends of the HE. This will involve an additional workmanship and cost.

Table 1. Physical properties of 310S stainless steel

Density (at 25°C)	Thermal Conductivity (at 100°C)	Melting Point	Specific Heat Capacity	Electrical Resistivity (at 25°C)
8 g.cm^{-3}	14.2 W.m^{-1}.°C^{-1}	1400°C	500 J.kg^{-1}.°C^{-1}	0.78 Ω.m

2.2. Electrical Insulation between Heating Coil and GT

The electrical insulating material between the HE and the GT in the GP should be thermally conductive. Moreover, it must be able to prevent oxidation of the heating wire, maintain its insulating property at high temperatures, and easily enter between the GT and the HE. In this study, magnesium oxide (MgO) was chosen as the material providing these properties. Its physical properties are shown in Table 2 [16]. Since MgO absorbs ambient moisture very quickly, it must be dried in the oven at about 100 °C before using. Unless the GT can be oxidized and be deformed resulting in shortening of the lifetime of the resistance element.

Table 2. Physical properties of MgO

Appearance	Melting point (°C)	Density (g.cm^{-3})	Thermal conductivity (W.m^{-1}.K^{-1})
White Powder	2830	3.58	45-60

2.3. The Insulator Ring

The insulation material inside the GT must not only avoid the conductivity between the positive lead and the vehicle's chassis (negative lead), but also withstand the motor temperature. In this study, a ring-insulation element is made of a polypropylene-based material which melting temperature is at about 160 °C.

2.4. Heating Element

The HE is used to heat the GT up to 800 °C - 1000 °C in optimum time. It consists of two resistance elements (HR and RR) connected in series showing in Fig.2. The heating temperature is provided by the HR, while the RR is used to limit the current in the circuit. The RR is essential to prevent the GT from reaching its melting temperature. The total resistance values of the HR and the RR must be initially small, so that the GT can quickly reach the desired temperature value. When a voltage is applied to these HEs, a large current flows through the first switch.

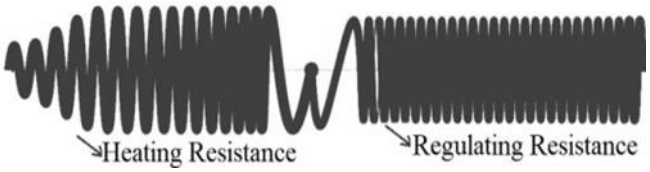

Figure 2. Scheme of heating element (HR and RR)

If the GPs are permanently switched on, they will draw more current than the battery (each GP draws a current of about 12 A), which shortens the life of the battery and negatively impacts the charge. In order to

overcome this drawback, the resistance of the HR should slightly change, while the resistance of the RR should increase more rapidly. In order to provide the necessary features in this work, it is considered suitable to use Kantal A [17] or D [18] as HR and Nickel 201 as RR. Physical properties of the materials used in the study are presented in Table 3.

Table 3. Physical properties of Kanthal A and Nickel 201

Items	Kanthal A	Nickel 201
Density (g.cm^{-3})	7.15	8.89
Electrical resistivity at 20°C (μΩ.m)	1.39	0.096
Melting point	1500 °C	1435 °C
Thermal conductivity (W.m^{-1}.K^{-1})	11 (at 50°C)	67.1 (at 100°C)
Temperature factor of resistivity at 800°C	1.05	0.46

3. Material and Method

The design parameters of the HR and RR must be determined appropriately to ensure that the GT reaches the required temperature. It is necessary to determine the cross-section and length of the RR and HR conductors and how they should be wrapped around the winding diameter. First of all, it is necessary to determine the total resistance value to reach the required temperature of the GT to be generated by the current that will flow through the HR. The amount of heat required to reach the desired temperature of the GT can be calculated from Eq. (1).

$$Q = m.c.\left(T_f - T_s\right) \quad (1)$$

Where; Q: the amount of heat (cal) to be supplied to the GT; m: mass of the heating zone (gr); c: specific heat of the GT (cal.gr^{-1}.°C^{-1}); Tf and Ts are the final and starting temperatures (°C) of the metal sheath. Initially, the HR must be able to generate this amount of heat in a very short time. From here, the amount of power that the HR must give every second can be calculated from Eq. (2).

$$P = 0,239 \cdot Q \quad \left(1\,W = 0,239\ cal/s\right) \quad (2)$$

The value of the HR to obtain the required heat can be calculated from Eq. (3).

$$R = U^2/P \quad (3)$$

Where; P is the amount of power that the HE must produce (W); U is the operating voltage of the HR (U is the battery voltage of the vehicle to be used). The length of the conductor required to obtain the heating resistance can be calculated from Eq. (4).

$$L = R \cdot A/\rho \quad (4)$$

Where; ρ is the resistivity (Ω.m), R is the electrical resistance of the material (Ω), L is the size of the material (m), A is the cross-sectional area of the material (m^2).

In practice, the operating voltages of the GPs are 5, 12 or 24 V. In Sea vehicles and small vehicles 5 V, automobiles 12 V, trucks, large vehicles such as TIR 24 V is used. For cars with a 12 V battery supply, an energy of about 150 W.s^{-1} must be provided in the GP cylinder. In this case, the total resistance of each HE can be calculated as R = 122/150 = 0.96 from Eq. (3). This study was done for 12 V GP used in automobile. When calculating the values for the HE, the heat transfer losses of the metal air heating and insulation materials were not taken into account at the beginning. In order to accurately estimate the value of the correction coefficient, a sample was first generated according to the data obtained from the calculations. A correction coefficient is obtained from the experimental results of the sample. The values of both HE and RR were re-determined with the obtained coefficient. The values obtained by taking the correction coefficient into account are given in Table 4.

Table 4. Technical values of HR and RR according to 12 V GP

Element	Material diameter (mm)	Number of turns	Winding diameter (mm)	Resistance (Ω; at 20 °C)	Resistance (Ω; at 800 °C)	Resistance (Ω; at 1100 °C)
HR	0.40	10	1.95	0.677	0.697	0.706
RR	0.25	26	2	0.319	1.530	1.797
HE	-	-	-	0.997	2.228	2.503

The resistance of the HR is slightly increasing while the one of RR increases abruptly with temperature. The change values of the total resistance 12 V GP of HE values depending on the temperature are given in Tab. 4.

The diffusion of heat along the GT induces the flow down of the current on both resistances; therefore, the temperature is decreasing with time. This is the reason why the melting temperature of the GT is never reached.

In Fig. 2, each of the elements used as resistors in the heating have a self-inductive value. It is well known that a solenoid inductor can be calculated from low frequencies, we can calculate the inductance using as Eq. (5) [19].

$$L = \frac{N^2 \cdot \mu_0 \cdot \mu r \cdot A}{l} \quad (5)$$

The electrical equivalent circuit of the GP is shown in Fig. 3.

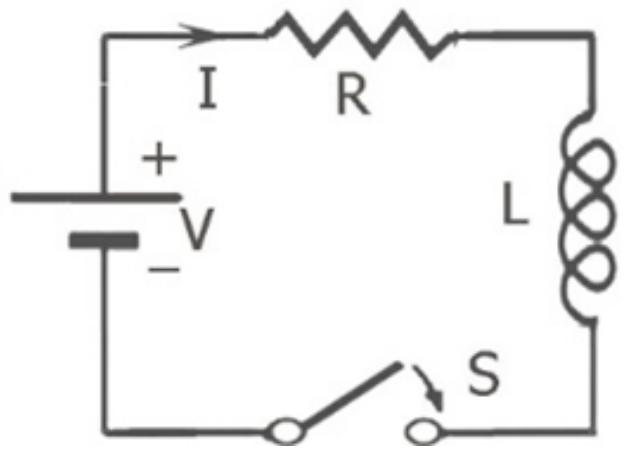

Figure 3. Electrical equivalent circuit of the GP

In Fig. 3, R represents the total resistance of the HEs and L represents the total inductance of the HEs. Using the modified Kirchhoff's rule for increasing current, dI/dt, the R-L circuit is described by the following differential Eq. (6).

$$V - I \cdot R - L\frac{dI}{dt} = 0 \quad (6)$$

Integrating over both sides and imposing the condition I(t=0) = 0, the solution to the differential equation is given in (7).

$$I(t) = \frac{V}{R}(1 - e^{-t \cdot L/R}) \quad (7)$$

In order to reach the V / R value in a very short time the circuit current must be as low as possible and R value as large as possible. If this time is too high, the heat generated by the HE in the GP will cause the heating tube to travel along the metal jacket to the body of the engine block. In this case, the heat to be delivered into the engine block will cause the desired temperature to reach a much longer time. As a result, the heat generated from the HTs cannot be used in a desired manner, which will cause unnecessary power retraction from the battery that will reduce the efficiency of the system and cause the vehicle to operate for a longer period of time. Reducing the minimum inductor value of the GT ensures that the current through the heating coil reaches its nominal value in a very short time, thus eliminating the above-mentioned drawbacks. The connection forms of the resistance wires to reduce the total inductor value as much as possible are shown in Fig. 4. Cumulatively Coupled Series Inductors (CCSI) are shown in Fig. 4(a), Differentially Coupled Series Inductors (DCSI) are shown in Fig. 4(b), and Proposed Method Inductors (PMI) are shown in Fig. 4(c).

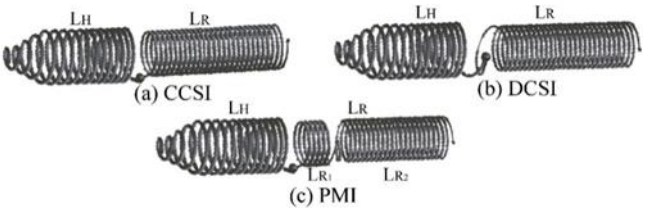

Figure 4. Winding patterns of HR and RR a) CCSI, b) DCSI, c) PMI

The process to reduce the total inductance value of the HR and the RR is as follows.

3.1. CCSIs

If the HR and the RR are wound in the same direction and are connected in series as shown in Fig. 4(a), the total ohmic resistances are R = RR + RH. Where: R: Total resistance, RR: Regulating coil of Resistance (Ω) and RH: Heating coil of Resistance (Ω). Because the form of winding does not affect the values of the HR and RR, other winding methods do not change the impedance values. Therefore, this equation will be the same for the three winding methods.

The total inductance is L = LR + LH. Where, LR is the regulating coil of inductor value (H) and LH is the heating coil of inductor (H). Since these resistors are placed in a conductive metal tube, mutual inductance between LR and LH occurs. In this study, the size and cross-section of the conductor to be used in the HR and RR are predetermined. As can be understood from the Eq. (4), while winding the resistors in the form of a coil, the winding radius should be kept as small as possible so that the inductor values are small. If the winding directions of the heating resistance wire and the balancing resistance wire are the same, the total inductance value can be calculated from Eq. (8) [20].

$$L\frac{dI}{dt} = L_R\frac{dI}{dt} + L_H\frac{dI}{dt} + 2M\frac{dI}{dt} \quad (8)$$

$$L=LR+LH+2M$$

Where; 2M represents the influence of coil LR on LH and likewise coil LH on LR. Eq. (8) can be written as in Eq. (9) in accordance with the operating parameters.

$$L_{Ta} = L_H + L_R + 2M_{HR} = L_H + L_R + 2\sqrt{L_H.L_R} \quad (9)$$

Where; $M_{HR} = \sqrt{L_H.L_R}$; $L_H = \mu N_H^2.A_H/l_H$; $L_R = \mu N_R^2.A_R/l_R$; $A_R = \pi D_R^2/4$; $A_H = \pi D_H^2/4$; $l_H = N_H s_H$; $l_R = N_R s_R$;

LTa; Total inductor of structures, LH: HR's inductor, LR: RR's inductor, MHR: Mutually inductance between HR and RR, NH: Turn number of heating resistance, NR: Turn number of RR, AH: Cross section area of HR (m^2), AR: Cross section area of RR (m^2), lH: Length of HRs (m), lR: Length of RRs (m), DH: Winding diameter of HR, DR: Winding diameter of RR, SH: Resistance diameter of HR, SR: Resistance diameter of RR. The inductor values for this winding type are given in Table 5. This method is not

suitable for winding because our aim in this study is to decrease the total inductor value. Because the mutually inductor value further increases the total inductor value.

3.2. DCSIs

If the HR is wound in one direction and the RR is wound in the opposite direction of the winding resistance and the series is connected as shown in Fig. 4(b). Since the winding directions of the HR wire (LH) and the RR wire (LR) are different, the total inductance value (LTb) can be calculated from the Eq. (10).

$$L_{Tb} = L_H + L_R - 2M_{HR} = L_H + L_R - 2\sqrt{L_H.L_R} \qquad (10)$$

The inductor values for this winding type are given in Table 5. Because our aim in this study is to reduce the total inductor value, this method may also be suitable for winding, because mutually reducing the value of the total inductor value of the inductors.

Table 5. 12 V GP Total inductance values of the HR and the RR in relation to the winding direction

Mutually inductors (μH)	CCSI (μH)	DCSI (μH)
0.196	0.700	0.112

3.3. PMIs

In this study, we aim to approximate the total inductor value to zero, so we propose a new form of winding as shown in Fig. 4(c) as a third method. As seen in Table 6, the total inductor value of the resistors decreases inversely with one another. If we want to reduce this value further, we can further reduce the total inductor value by reversing some of the RR in itself. In this technique, the heating coil is wound with the winding direction and part of the RR coil being in the same direction. The remaining part of the RR coil is wound in the opposite direction to the first part. When LR in Eq. 10 is substituted by LR=LR1+LR2−2√(LR1.LR2), the total inductance value (LTc) presented in Eq. (11) can be obtained.

$$L_{Tc} = L_H + \left(L_{R1} + L_{R2} - 2\sqrt{L_{R1}.L_{R2}}\right) - 2\sqrt{L_H.\left(L_{R1} + L_{R2} - 2\sqrt{L_{R1}.L_{R2}}\right)} \qquad (11)$$

$$L_{R1} = \mu N_{R1}^2.A_R/l_{R1};\ \ L_{R2} = \mu N_{R2}^2.A_R/l_{R2}$$

LTc; Total inductor of proposed structures, LR1: First part of RR's inductor in proposed model, LR2: Second part of RR's inductor in proposed model.

The purpose here is to set the mutual impedance value to be M = (LR + LH) / 2. Table 6 of the proposed method gives the mutually inductor values for the 12V HR to be formed when the RR is wound in the same direction as the 5-turn HR. The table for the recommended method for 12V GP is given in Table 6.

Resistance values and total inductor values are given in Table 7. Depending on the temperature of 12V GP from Eq. (5), it can be said that the value of the inductor does not significantly depend on the temperature.

Table 6. 12 V GP Inductor values for the proposed method

Resistance	Material diameter (mm)	Winding diameter (mm)	Number of turns	Winding and direction	Mutually Inductors (μH)
HR	0.40	1.95	10	10 same direction	0.0938
RR	0.25	2	26	21 reverse direction	0.3358
RR	0.25	2	26	5 same direction	0.0746

Table 7. Resistance values and total inductor values depending on the temperature of 12 V GP

Temperature (°C)	HR (Ω)	RR (Ω)	HE (Ω)	CCSI (μH)	DCSI (μH)	PMWI (μH)
20	0.677	0.319	0.997	0.896	0.111	≅0
800	0.697	1.530	2.228	0.896	0.111	≅0
1100	0.706	1.797	2.503	0.896	0.111	≅0

Conductor cross-sections of HR and RR are different and are made from different materials. The series connection of the two groups of winding is performed by the welding method shown in Fig. 5(a). The welding process was performed with the laser diode pumped Nd:YAG laser device shown in Fig. 5(b) because the conductor's cross-sections are small and require precise welding operation [21-22].

In this study, the HE was made in the form of a replaceable tube as shown in Fig. 6. Thus, the GP can be easily replaced without removing the part that is mounted on the cylinder block. Therefore, both labor and material savings are provided.

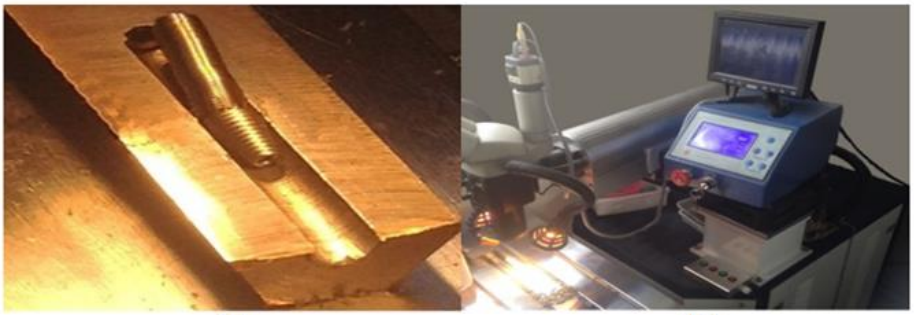

Figure 5. a) Welding of resistance wires b) Laser device

Figure 6. GP's mounting style for changing the HE

3.4. Experimental GP Test Setup

In order to obtain the experimental test results of the designed and manufactured GP, the test setup block diagram is given in Fig. 7.

The assembly of the manufactured sample GP to the test assembly is shown in Fig. 8(a). The voltage and current values applied to the GP the Human Machine Interface (HMI) screen display is shown in Fig. 8(b). Fig. 8(c) shows the thermal camera image of the end of the GP.

Pyrometer shown in Fig. 8(a) is used for GP tip temperature measurement in this study.

One of the pyrometers (Dias Company's Pyrospot DG 10N / DG 10NV) was used to measure the temperature distribution of the GP end region as shown in Fig. 8(a). This pyrometer has display output and analog output. As can be seen in Fig. 8(c), the temperature distribution of the measurement area can be measured from a display connected to the screen output. The GP tip temperature measurement data was transferred from this pyrometer analogue output to the Programmable Logic Controller (PLC).

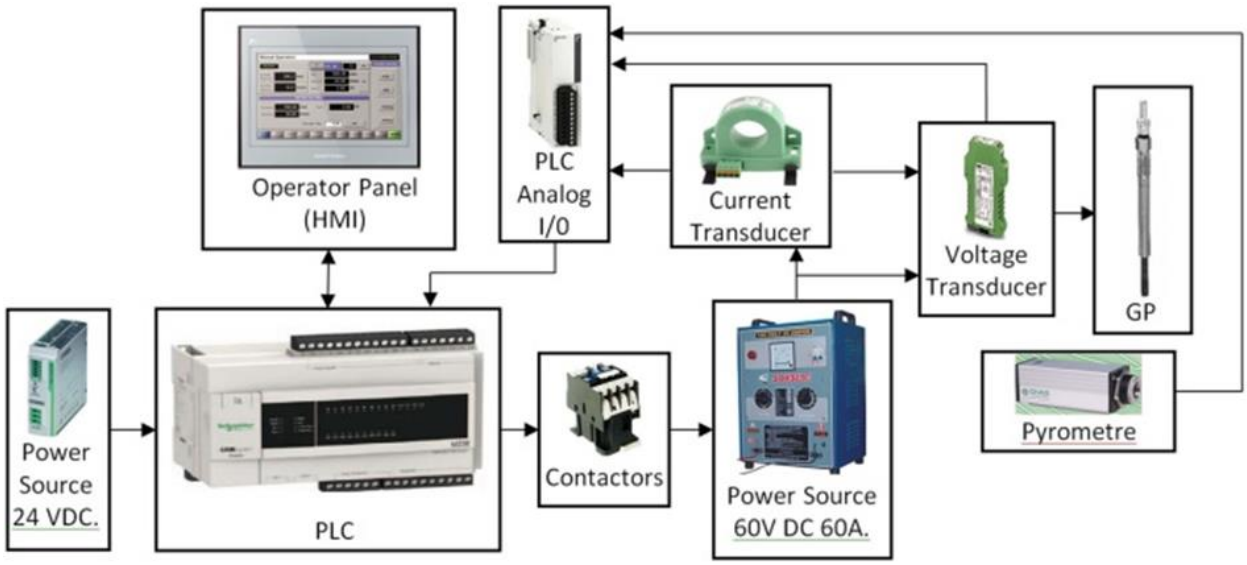

Figure 7. Block diagram of test setup

(a) (b) (c)

Figure 8. a) Test setup, b) HMI image of test data, c) Thermal camera image

4. Results and Discussion

A 12 V GP was manufactured with three winding techniques, corresponding to the parameters given in the study (Tab. 4 and Tab. 6). The variation of the current and total power consumption of the HE is shown in Fig. 9(a) and Fig 9(b) respectively.

In the proposed novel method, which is understandable from the interpretations of the graph, the current reaches the nominal value very quickly. By using this proposed novel method, it is possible to reach the nominal value of the current in a very short time like 1μs by reducing the total inductor value of the HEs as much as possible. In this case, the temperature of the zone where the glow tube HR is located can reach 800-1000 °C in a short time like 6s without allowing the heat obtained from the HR to spread through the GT. In this study, it was tried to approximate the total value to zero by considering the series connected inductors in the mutually inductor values. Whatever is done, this value cannot be really zero due to even electric power cables that feed GPs have an inductive value. In this study, it was tried to reduce this value as much as possible by the winding method developed.

The pulling of the total inductor value of the GP resistors may be possible by reducing the coil surface area as understood from the Eq. (4). However, it is possible to reduce the surface area of the HR only with a winding of smaller diameter. In this case, it is difficult to transfer the heat from the HR to the GT trough. In this case, the result is that the material used for making the HR reaches the melting point of the material and deteriorates. Therefore, this method is not preferred in this study.

Experimental images of the proposed method and the other methods of GP at the same time are given in Fig. 8. GPs produced with these three methods have been tested together, after applying 12 A at start and waiting 6 s, it can be seen that the heating is low for GP prepared with CCSI, while highly heated but short area is observed with DCSI method and finally highly heated on large area is observed with PMI. Samples are presented in Fig. 10.

In order to obtain the test results according to the three methods mentioned in this study, 4 pieces of GP according to each method were manufactured. The test results of the GPs were obtained as a result of testing the experimental setup one by one. The test results were obtained using the experimental setup given in Fig. 8. When we applied voltage to the GP's, we started up a chronometer in PLC and recorded the instantaneous temperature time change values depending on the time with the pyrometer which we mounted on the test system. We selected sampling time of 50 ms for this study. The temperature change of each GP was recorded in PLC for a sampling time of 0.5 s. The averages of the test results obtained for each method are shown in the graph of Fig. 11. There are very small temperature changes between GP's temperatures. This can be interpreted as the sum of a number of errors that can occur up to the time when the resistive wire section used in the production stage of the product is not homogeneous, the delay in PLC sampling time and etc. As can be understood from Fig. 11, at the end of 5 seconds, the GP tip temperature was 670 °C at the CCSI technique, 800 °C at the DCSI technique, and 850 °C at the PMI technique.

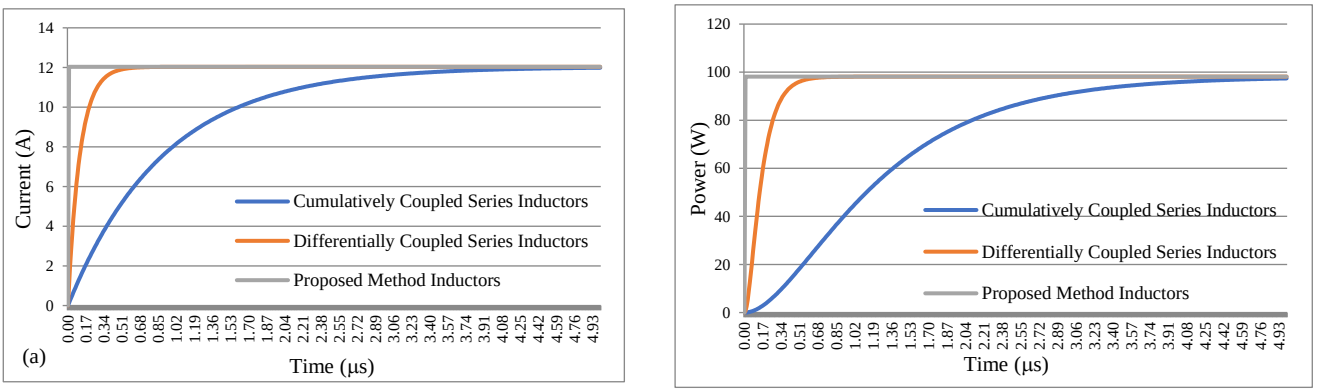

Figure 9. Shows the time-dependent; a) Current b) total power consumption on HE of 12 V GPs manufactured according to three methods

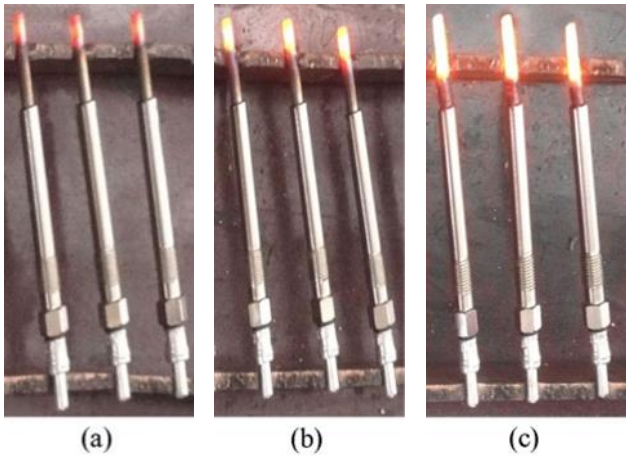

Figure 10. GP of; (a) CCSIs, (b) DCSIs, (c) PMIs.

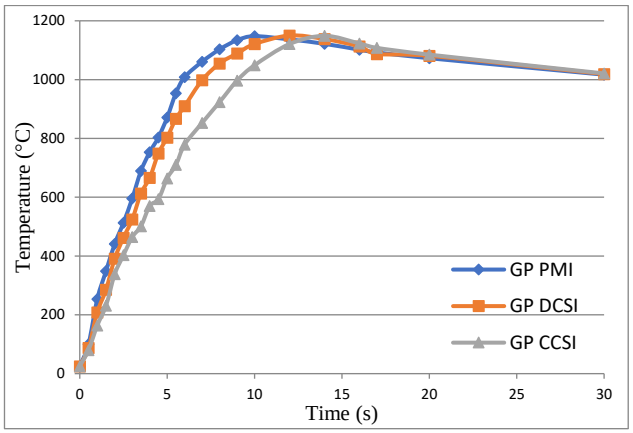

Figure 11. Change of the tip temperatures of the four GP produced by three methods depending on the time

5. Conclusion

In this study, the work to be done on the product was investigated and the results were observed experimentally in order to reduce the duration of warming and to produce standard GP's. With the product improvement work made, the electrical properties of the GP's are made identical and the production GP are provided at 850 ° C for 5 seconds. The standard product is obtained to ensure the combustion of each cylinder block at the same time, preventing greenhouse gas emissions from causing unnecessary mechanical knocking and unnecessary greening of the environment. During the delay in achieving the desired temperature of the GP's during the required time, the heat generated by the GP is absorbed by the cylinder volume, causing the GP to heat up longer and to consume more power from the battery. Thanks to the work done, optimal heat is obtained from reaching the optimum temperature during the optimum time, which prevents unnecessary power consumption from the battery and shortening the battery life. Considering that there are millions of vehicles in the world, the positive effect of any improvement in exhaust emissions on global warming is so important that it cannot be ignored.

Deterioration of the GP's is usually caused by exposure of the outer surface of the HE to corrosive effects or breakage of the resistance material contained therein. In the event of a malfunction in this work, the GP is replaced by a tube, which requires the most workmanship to replace it. In this case, it is manufactured in such a way that this tube can be easily changed so that maintenance can be done quickly and easily, and the service cost are reduced by 60%. The part of the GP mounted on the engine block has been reduced to prevent the adverse effects on the environment.

Acknowledgement

This study was supported by TUBITAK 1507, 7131171under Project Number 3080487 from the Industry R&D support program, and by the Scientific Research Projects (BAP) Coordinatorship Office of Necmettin Erbakan University.

Author contributions

Muciz Özcan: Determining the aim and creating the methodology of the study and coordinating the study. Conducting experiments and interpreting the results obtained. **Muhammed Fahri Ünlerşen:** Calculating the indicator value and helping with some calculations. **Mehmet Şen:** Conducting experiments and interpreting the results obtained. Writing-Reviewing and Editing the manuscript.

Conflicts of interest

The authors declare no conflicts of interest.

References

1. Özcan, M., & Günay, H. (2013). Control of diesel engines mounted on vehicles in mobile cranes via CAN bus. Turkish Journal of Electrical Engineering and Computer Science, 21(Sup. 2), 2181-2190.
2. Siskos, P., Capros, P., & De Vita, A. (2015). CO_2 and energy efficiency car standards in the EU in the context of a decarbonisation strategy: A model-based policy assessment. Energy Policy, 84, 22-34.
3. Peng, B. B., Fan, Y., & Xu, J. H. (2016). Integrated assessment of energy efficiency technologies and CO_2 abatement cost curves in China's road passenger car sector. Energy conversion and management, 109, 195-212.
4. Last, B., Houben, H., Rottner, M., & Stotz, I. (2008, March). Influence of modern diesel cold start systems on the cold start, warm-up and emissions of diesel engines. Paper presented in Proceedings of the 8th Stuttgart International Symposium, Stuttgart, Germany.
5. Weilenmann, M., Favez, J. Y., & Alvarez, R. (2009). Cold-start emissions of modern passenger cars at different low ambient temperatures and their evolution over vehicle legislation categories. Atmospheric environment, 43(15), 2419-2429.
6. Qi, D. H., Bian, Y. Z., Ma, Z. Y., Zhang, C. H., & Liu, S. Q. (2007). Combustion and exhaust emission characteristics of a compression ignition engine using

liquefied petroleum gas–diesel blended fuel. Energy conversion and management, 48(2), 500-509.
7. Kökkülünk, G., Akdoğan, E., & Ayhan, V. (2013). Prediction of emissions and exhaust temperature for direct injection diesel engine with emulsified fuel using ANN. Turkish Journal of Electrical Engineering & Computer Sciences, 21(Sup. 2), 2141-2152.
8. Mrzljak, V., Medica, V., & Bukovac, O. (2017). Quasi-dimensional diesel engine model with direct calculation of cylinder temperature and pressure. Tehnički vjesnik, 24 (3), 681-686. https://doi.org/10.17559/TV-20151116115801.
9. He, B. Q. (2016). Advances in emission characteristics of diesel engines using different biodiesel fuels. Renewable and Sustainable Energy Reviews, 60, 570-586.
10. Barna, L., & Lelea, D. (2017). Low pressure injection of oxyhydrogen in turbocharged compression ignition engines. Tehnički vjesnik, 24 (Supplement 2), 287-294. https://doi.org/10.17559/TV-20150921183805.
11. Payri, F., Broatch, A., Salavert, J. M., & Martín, J. (2010). Investigation of Diesel combustion using multiple injection strategies for idling after cold start of passenger-car engines. Experimental Thermal and Fluid Science, 34(7), 857-865
12. Endiz, M. S., Özcan, M., Erişmiş, M. A., Yağcı, M., & Günay, H. (2015). The simulation and production of glow plugs based on thermal modeling. Turkish Journal of Electrical Engineering & Computer Sciences, 23(Sup. 1), 2197-2207.
13. Sakunthalai, R. A., Xu, H., Liu, D., Tian, J., Wyszynski, M., & Piaszyk, J. (2014). Impact of cold ambient conditions on cold start and idle emissions from diesel engines (No. 2014-01-2715). SAE Technical Paper.
14. Bosch, R., & Peter, (Tr.) G. (1996). Automotive handbook. Society of Automotive Engineers, US.
15. Cobb, H. M. (2010). The history of stainless steel. ASM International.
16. Lee, B., Liu, J. Z., Sun, B., Shen, C. Y., & Dai, G. C. (2008). Thermally conductive and electrically insulating EVA composite encapsulants for solar photovoltaic (PV) cell. eXPRESS Polymer Letters, 2(5), 357-363.
17. Kanthal, A. B. (2008). Thermostatic bimetal handbook. Hallstahammar, Sweden.
18. Davis, J. R. (Ed.) (2000). Nickel, cobalt, and their alloys. ASM international.
19. Soohoo, R. (1979). Magnetic thin film inductors for integrated circuit applications. IEEE Transactions on Magnetics, 15(6), 1803-1805.
20. Nilsson, J. W., & Riedel, S. A. (2015). Electric Circuits. 10th ed. New Jersey, USA: Pearson.
21. Siewert, T., Samardžić, I., Kolumbić, Z., & Klarić, Š. (2008). On-line monitoring system-an application for monitoring key welding parameters of different welding processes. Tehnički vjesnik, 15(2), 9-18.
22. Ozcan, M. (2003). The design and application of an effective power supply for Nd:YAG laser used on machining of various materials. Doctoral Thesis, Selçuk University, Council of Higher Education Thesis Center, Konya, 157p